

1 **Appendix**

2 **Slowdown of growth controls cellular differentiation**

3 Jatin Narula\*<sup>1</sup>, Anna Kuchina\*<sup>2</sup>, Fang Zhang<sup>2</sup>, Masaya Fujita<sup>3</sup>, Gürol M. Süel‡<sup>2</sup> and Oleg A.  
4 Igoshin‡<sup>1</sup>

5 <sup>1</sup>Department of Bioengineering, Rice University, <sup>2</sup>Division of Biological Sciences, UCSD,

6 <sup>3</sup>Department of Biology and Biochemistry, University of Houston

7 —

8 ‡ authors to whom correspondence should be addressed

9

10

11 **1. Appendix Figure 1**

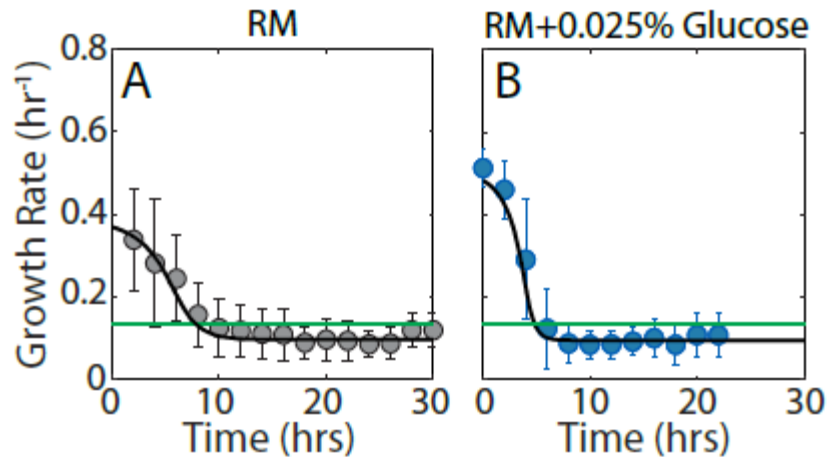
12 **2. Appendix Tables A1-A3**

13 **3. Appendix Text A1: Mathematical Model of Sporulation Phosphorelay**

14 **4. Appendix Text A2: Population Dynamics Model of Growth and Sporulation**

15 **5. Appendix References**

16



17

18 **Appendix Figure 1. Effect of nutrient availability on growth slowdown and sporulation**  
 19 **dynamics.**

20 **A.** Dynamics of growth slowdown in normal starvation media (RM). Gray circles and errorbars show the  
 21 mean and standard deviations respectively of the growth rate of a colony of cells in RM. In RM substrate  
 22 availability is low from the start of the experiment. As a result, cells grow slowly and accordingly nutrient  
 23 levels are depleted gradually until cells cross the growth threshold for sporulation (green line) around 10  
 24 hours into the experiment. Fitting this data (black curve) shows that these growth rate dynamics can be  
 25 explained by a simple population dynamics model for substrate amount and number of cells (see  
 26 Supplementary Text S2 for details).

27 **B.** Dynamics of growth slowdown with increased initial nutrients (RM+0.025% glucose). The population  
 28 dynamics model predicts that growth rate dynamics are sensitive to initial nutrient availability. Glucose  
 29 addition at the start of the experiment leads to the high initial growth rate and postpones starvation.  
 30 However, subsequently, the increased number of cells results in rapid depletion of nutrients and decrease  
 31 in growth rate (black curve). As a result, cells cross the growth threshold (green line) for sporulation  
 32 earlier around 7 hours into the experiment. Experimental measurements of growth dynamics (blue circles)  
 33 in RM+0.025% glucose confirmed the model predictions. Blue circles and errorbars show the mean and  
 34 standard deviations respectively.

35

36 **2. Appendix Tables**

37

38 **Table A1.** *B. subtilis* strains used in this study

39

<i>B. subtilis</i> strains as referred in the article	<i>B. subtilis</i> strain number	Genotype	Used in Figures
“Wildtype”, WT	AK151	<i>AmyE::P<sub>spo0A</sub>-yfp, P<sub>comG</sub>-mCherry (Sp<sup>R</sup>) SacA::P<sub>spoIIIR</sub>-cfp (Cm<sup>R</sup>)</i>	Fig. 2D; Fig. S2; Fig. S3
	TC669	<i>AmyE::P<sub>hsp</sub>-yfp (Sp<sup>R</sup>)</i>	Fig. 2A; Fig. S1D-F
	AK2161	<i>P<sub>spoIIIR</sub>-YFP, P<sub>spo0A</sub>-CFP, pDG148-P<sub>tpsD</sub>-mCherry</i>	Fig. 1C-F; Fig. 3; Fig. S1H
	AK456	<i>AmyE::P<sub>spo0F</sub>-yfp (Sp<sup>R</sup>)</i>	Fig. S1A-C, G
	MF929	<i>KinA::P<sub>kinA</sub>-kinA-gfp (Kan<sup>R</sup>)</i>	Fig. 5CDE; Fig. S6
	AK2261	<i>AmyE::P<sub>hsp</sub>-DnaN-YFP (Sp<sup>R</sup>) pHP13- P<sub>spo0A</sub>-cfp, P<sub>comG</sub>-mCherry (Erm<sup>R</sup>)</i>	Fig. S1I
<i>iTrans-0F</i>	AK2092	<i>AmyE::P<sub>hsp</sub>-Spo0F (Sp<sup>R</sup>) SacA:: P<sub>spoIIIR</sub>-yfp (Cm<sup>R</sup>) GltA::P<sub>spo0F</sub>-Spo0F (Pm<sup>R</sup>) pHP13- P<sub>spo0A</sub>-cfp (Erm<sup>R</sup>) Spo0F:: kan (Kan<sup>R</sup>)</i>	Fig. 4D-I
Inducible KinA	MF2840	<i>KinA::P<sub>hsp</sub>-kinA-gfp (Cm<sup>R</sup>) (Kan<sup>R</sup>)</i>	Fig. 5CDE; Fig. S6
Sda deletion	F47-1	<i>sda::cm (Cm<sup>R</sup>), AmyE::P<sub>spo0A</sub>-yfp, P<sub>comG</sub>-mCherry (Spec)</i>	Fig. S7

40

41

42 **Table A2.** Parameter values used for gene regulatory interactions in the model of sporulation phosphorelay.

43

44

Reaction	Rate	Values
→ KinA	$v_{kinA} = v_{kinA}^0 + v_{kinA}^{max} \frac{[S]^m}{K_{kinA}^m + [S]^m}$	$v_{kinA}^0 = 0.9 \mu M \text{ hr}^{-1}$ , $v_{kinA}^{max} = 1.5 \mu M \text{ hr}^{-1}$ $K_{kinA} = 0.025 \mu M$ , $m = 1$
→ 0F	$v_{0F} = v_{0F}^0 + v_{0F}^{max} \frac{[S]^m}{K_{0F}^m + [S]^m}$	$v_{0F}^0 = 0.15 \mu M \text{ hr}^{-1}$ , $v_{0F}^{max} = 3 \mu M \text{ hr}^{-1}$ $K_{0F} = 0.15 \mu M$ , $m = 2$
→ 0B	$v_{0B}$	$v_{0B} = 0.3 \mu M \text{ hr}^{-1}$
→ 0A	$v_{0A} = v_{0A}^0 + v_{0A}^{max} \frac{[S]^m}{K_{0A}^m + [S]^m}$	$v_{0A}^0 = 1.5 \mu M \text{ hr}^{-1}$ , $v_{0A}^{max} = 6 \mu M \text{ hr}^{-1}$ $K_{0A} = 0.35 \mu M$ , $m = 2$
→ Rap	$v_{rap}$	$v_{rap} = 0.075 \mu M \text{ hr}^{-1}$
→ 0E	$v_{0E}$	$v_{0E} = 0.03 \mu M \text{ hr}^{-1}$

45

46

47

48

49 **Table A3.** Parameter values used for the population dynamics model of growth dynamics during  
 50 starvation.  
 51

Parameter	Description	Value
$v_m$	Maximum growth Rate	$1.13 \text{ hr}^{-1}$
$K_m$	Half-maximal substrate concentration	0.82
$k_d$	Maximum sporulation rate	$0.1 \text{ hr}^{-1}$
$K_S$	Half-maximal substrate concentration for sporulation	0.5
$m$	Hill-exponent for sporulation rate	3.5
$\gamma$	Substrate yield	0.02 substrate amt./cell
$N_0$	Initial Cell Number	SM: 5, SM+0.025% Glucose: 5
$S_0$	Initial Substrate Concentration	SM: 0.44, SM+0.025% Glucose: 0.72

52

53

54

### 55 3. Appendix Text A1: Mathematical Modeling Methods

56 *Derivation of the dependence of protein concentrations on growth rate (Eq. [1])*

57 To derive the Eq. [1] from the main text describing the dependence of protein  
58 concentration (C), on growth rate ( $\mu$ ) we started with differential equations for protein  
59 molecule number (N) including production and degradation terms and for exponential  
60 growth of cell volume (V):

$$\begin{aligned} \frac{dN}{dt} &= P - k_{\text{deg}}N \\ \frac{dV}{dt} &= \mu V \end{aligned}$$

62 In the first equation, we include protein production (rate P) and degradation (rate  $k_{\text{deg}}$ ).  
63 The second equation describes the exponential increase in cell volume with growth rate  
64  $\mu$ . Using these equations and definition for concentration  $C=N/V$ , we can derive the rate  
65 of change of C:

$$\frac{dC}{dt} = \frac{d}{dt} \left( \frac{N}{V} \right) = \frac{1}{V} \frac{dN}{dt} - \frac{N}{V^2} \frac{dV}{dt} = \frac{1}{V} (P - k_{\text{deg}}N) - \frac{N}{V} \mu = \frac{P}{V} - (\mu + k_{\text{deg}})C$$

67 At steady state this equation result in the postulated dependence of C on growth rate  
68 (Eq. [1] in the main text)

69  
70 *Phosphorelay network model*

71  
72 To investigate the dependence of 0A activity on cell growth rates we extended a  
73 previous mathematical model of sporulation phosphorelay network (Narula, Kuchina et  
74 al. 2015). This model used ordinary-differential equations describing concentration of  
75 the phosphorelay proteins and their complexes as a function of time to provide a  
76 deterministic description of the phosphorelay network response.

77  
78 Our model can be subdivided into the following two parts: (i) the post-translational  
79 interactions that describe the phosphorylation/dephosphorylation of phosphorelay  
80 species and (ii) the transcriptional feedback interactions that control the expression of  
81 the phosphorelay proteins.

82  
83 Post-translationally, the activity of the sporulation master regulator is controlled by the  
84 sporulation phosphorelay through phosphorylation/dephosphorylation reactions (Fig.  
85 1B). Specifically, phosphoryl groups are transferred from the major sporulation kinase  
86 KinA to Spo0A (0A) via the phosphotransferases Spo0B (0B) and Spo0F (0F) (Hoch

87 1993, Eswaremoorthy, Duan et al. 2010). Phosphorylated *OF* (*OF~P*) and *OA* (*OA~P*) are  
 88 subject to negative regulation by phosphatases *Rap* and *Spo0E* (*OE*), respectively. All  
 89 post-translational reactions were modeled exactly as in (Narula, Kuchina et al. 2015)  
 90 with mass-action kinetics and the rate constants that were estimated from the *in vitro*  
 91 measurements of phosphorelay kinetics (Grimshaw, Huang et al. 1998).

92  
 93 Transcriptionally, the production of the phosphorelay genes *kinA*, *OF*, and *OA* is  
 94 regulated by *OA~P* (Fig. 1B) both directly and indirectly (via  $\sigma^H$ ), thereby forming multiple  
 95 feedback loops (Weir, Predich et al. 1991, Fujita and Sadaie 1998). For modeling the  
 96 expression of phosphorelay proteins, we again followed (Narula, Kuchina et al. 2015)  
 97 and assumed that rates of transcription can be modeled with appropriate Hill-functions.  
 98 To model the delay induced by indirect feedback we assumed that *OA~P* levels control  
 99 the expression an intermediate regulator *S* which in turn controls the transcription of  
 100 *kinA*, *OF*, and *OA* (similar to (Levine, Fontes et al. 2012)). The regulation of *kinA*, *OF*, and  
 101 *OA* transcription intermediate regulators was modeled with the generic Hill-function:

$$v_p = v^0 + v^{\max} \frac{[OA\sim P]^m}{K^m + [OA\sim P]^m}$$

102  
 103 Here  $v^0$  and  $v^{\max}$  represent the basal and maximal rate of transcription, respectively. *K*  
 104 and *m* represent the half-maximal binding constant and the Hill-exponent, respectively.  
 105 For simplicity, the rate of expression of the intermediate regulator was assumed to be  
 106 linearly dependent on  $v_p(OA\sim P)$ . For *spo0B*, *spo0E* and *rap* we assumed constant rates  
 107 of transcription. The specific rate expressions and parameter values used are described  
 108 in Table A2.

109  
 110 For the simulations of the inducible *KinA* strains (Figures 3CD), the *kinA* expression rate  
 111  $V_{kinA}$  was independent of *OA~P* and varied between 0  $\mu\text{Mhr}^{-1}$  and 5  $\mu\text{Mhr}^{-1}$ . For the  
 112 simulations of the *iTrans-OF* strain (Figures 4BC), the expression rate for the origin-  
 113 proximal *P<sub>hsp</sub>-OF* was independent of *OA~P* and fixed at 0.7  $\mu\text{Mhr}^{-1}$ . The protein  
 114 degradation rate was constant for all proteins and was fixed at 0.3  $\text{hr}^{-1}$ .

115  
 116 *Growth and gene copy number dependence of transcription rate*

117  
 118 The rates of expression of all genes in the model were assumed to be proportional to  
 119 the gene copy number and cell growth rate according to the following equation:

120  
 121 
$$v = g * v_p / F(\mu)$$

122 Where  $v$  is the actual rate of gene expression,  $v_p$  represents the expressions described  
123 for each gene in Table A2,  $g$  is the gene copy number and  $F(\mu)$  is a proportionality factor  
124 that models the effect of changes in cell size depending on the growth rate  $\mu$ .  $F(\mu)$  is  
125 normalized such that  $F=1$  for cells with doubling time of 1 hour ( $\mu=\log(2) \text{ hr}^{-1}$ ). We used  
126 the following phenomenological expression for  $F(\mu)$ :

$$127 \quad F(\mu)=a*\exp(b*\mu)+c$$

128 The values for  $a$ ,  $b$  and  $c$  were determined by fitting the data for change in cell length at  
129 division as a function of growth rate (Fig. EV1H). We found that  $a=0.690$ ,  $b=0.689$  and  
130  $c=0.745$ .

131

### 132 *Simulations*

133 All simulations of the phosphorelay response (Figs. 2, 5 and EV5) were done using the  
134 *ode15s* solver of MATLAB and a decreasing series of cell-cycle growth rates ( $\mu$ ) to  
135 mimic the starvation response in the experiments (compare Figs. 1 and 2B).

136 The cell-cycle durations,  $T_{\text{cyc}}$  were fixed based on the growth rates:

$$137 \quad T_{\text{cyc}}=\log(2)/\mu \text{ hrs}$$

138 The DNA replication period duration  $T_{\text{rep}}$ , was also assumed to be growth rate  
139 dependent and we used the following phenomenological expression for  $T_{\text{rep}}$ :

$$140 \quad T_{\text{rep}}=0.78+0.15/\mu \text{ hrs}$$

141 The values of the coefficients in the above equation were determined by fitting the data  
142 for change in DNA replication periods as a function of growth rate (Fig. EV1I). To  
143 identify DNA replication windows in time-lapse experiments we expressed a fluorescent  
144 DnaN-YFP fusion protein from the IPTG inducible  $P_{\text{hsp}}$  promoter and used the same  
145 quantification procedure as that described in (Narula, Kuchina et al. 2015).

146 For simplicity, replication was assumed to start immediately after cell-division.

147 All origin proximal genes ( $OF$ ,  $P_{\text{hsp}}-OF$  in *iTrans-OF* and  $P_{OA}$  reporters) were assumed to  
148 be replicated at the start of the DNA replication period and all terminus proximal genes  
149 ( $kinA$ ,  $OB$ ,  $OA$ ,  $OF$  in *iTrans-OF* and  $P_{\text{hsp}}-kinA-gfp$  in the inducible KinA strain) were  
150 assumed to be replicated at the end of the DNA replication time-window.

151 For the signal dependent KinA activity hypothesis (Fig. 5A and Fig. EV4BDF), the KinA  
152 autophosphorylation rate,  $k_p$  was assumed to depend on the growth rate:

$$153 \quad k_p=1+12/((5.8*\mu)^4+1) \text{ hr}^{-1}$$

154 For the signal independent KinA activity hypothesis (Fig. 5B and Fig. EV4CEG), the  
155 KinA autophosphorylation rate,  $k_p$  was fixed at  $12 \text{ hr}^{-1}$  and assumed to be independent  
156 of growth rate.

157

### 158 *Dose responses of 0A~P pulse amplitudes*

159 Under both signal-dependent and signal-independent KinA activity hypotheses, the  
160 0A~P pulse amplitude, growth rate and KinA concentration during each cell-cycle were  
161 calculated from these simulations to determine the 0A~P pulse amplitude vs growth rate  
162 (Fig. 2D and Fig. EV4DE) and 0A~P pulse amplitude vs KinA concentration (Fig.  
163 EV4FG) dose response relationships.

164 To calculate the growth rate and KinA thresholds the 0A~P threshold was fixed at  $0.9$   
165  $\mu\text{M}$  and the dose response relationships were used to find the corresponding growth  
166 rate and KinA level. In the inducible KinA strain, the KinA and growth thresholds were  
167 calculated at different *kinA* production rates ( $V_{\text{kinA}}$ ) to determine the interdependence of  
168 KinA and growth thresholds under the signal dependent and signal independent KinA  
169 activity hypotheses (Fig. 5AB).

170

### 171 *Sensitivity of 0A~P pulse amplitudes*

172 To calculate the sensitivity of 0A~P pulse amplitudes to variations in the phosphorelay  
173 protein levels (Fig. 2C) we tested the effect of increasing the production rate of the  
174 proteins on the 0A~P pulse amplitude. For each phosphorelay protein  $p$ , the production  
175 rate  $v_p$ , was increased by  $\Delta=10\%$  and then the 0A~P pulse amplitude  $[0A\sim P]_{\Delta}$ , was  
176 calculated at the growth rate  $\mu=0.15\text{hr}^{-1}$  (corresponds to the  $[0A\sim P]_{\text{WT}}=0.9\mu\text{M}$  – the  
177 sporulation threshold in our wildtype simulations). The normalized sensitivity of 0A~P  
178 pulse amplitudes to each phosphorelay protein  $p$  was then calculated using the  
179 following equation:

$$180 \quad S_p = \frac{[0A\sim P]_{\Delta} - [0A\sim P]_{\text{WT}}}{\Delta * [0A\sim P]_{\text{WT}}}$$

181

### 182 *Matlab code for growth dependent phosphorelay model simulations*

183

```
184 function PhosphorelayGrowthModel  
185 clc;clear;format('compact');  
186 close all;  
187  
188 %Set Phosphorelay Parameters
```



```

189 pars=setpars;
190
191 %Calculate Initial Conditions
192 xii=zeros(1,20);
193 par1=pars;
194 par1(20)=0.5;par1(36)=2*pars(36);
195 [~,y]=ode15s(@eqnsint,[0 2e3],xii,[],par1);xi=y(end,:);
196
197 tsers=[];t0=0;ts=[];y1=[];kgrowths1=[];tss=[];tdivs=[];
198
199 % Set Growth History
200 kgs=logspace(log10(0.05),log10(0.5),12);
201 kgrowths=[0.5*ones(1,3),fliplr(kgs)];nrep=numel(kgrowths);
202
203 funtser=@(t,t2,st) logical(mod(t,st)>=0).*logical(mod(t,st)<t2);
204
205 %Growth dependence of gene expression rate
206 fvk=@(x) (3.466*exp(-log(2)./1)+3.743)./(3.466*exp(-log(2)./x)+3.743);
207 vind=[1 2 3 4 21 24 27 30 31];
208
209 %Growth dependence of DNA replication duration
210 fRepDuration=@(x) (0.15./x+0.78);
211
212 for i=1:nrep
213     par1=pars;
214     CellCycDuration=log(2)/kgrowths(i);
215     RepDuration=fRepDuration(kgrowths(i));
216     par1(20)=kgrowths(i);
217     par1(vind)=pars(vind)*fvk(kgrowths(i));
218
219     ts1=linspace(0,CellCycDuration,round(CellCycDuration)*100)';
220     tser=funtser(ts1,RepDuration,CellCycDuration);
221     tss=[tss;t0+ts1];tsers=[tsers;tser];
222     tdivs=[tdivs t0+CellCycDuration];
223
224     par2=par1;
225     par2(36)=2*pars(36);
226     [t,y]=ode15s(@eqnsint,[t0,t0+RepDuration],xi,[],par2);xi=y(end,:);
227
228     ts=[ts;t];y1=[y1;y];kgrowths1=[kgrowths1;kgrowths(i)*ones(size(t))];
229
230     if CellCycDuration>RepDuration
231         par2=par1;
232         par2([35 36])=2*pars([35 36]);
233
234     [t,y]=ode15s(@eqnsint,[t0+RepDuration,t0+CellCycDuration],xi,[],par2);
235     xi=y(end,:);
236
237     ts=[ts;t];y1=[y1;y];kgrowths1=[kgrowths1;kgrowths(i)*ones(size(t))];
238     end

```

```

239
240     t0=t(end);
241 end
242
243 Ap=y1(:,13);
244
245 figure(1)
246 subplot(211)
247 map=0.5;box on;
248 area(tss,map*tsers,'FaceColor',0.9*ones(1,3),'EdgeColor','none');hold
249 on;
250 plot(ts,kgrowthsl,'b');ylim([0 map]);xlim([0 max(ts)]);
251 line([tdivs;tdivs],[zeros(1,numel(tdivs));map*ones(1,numel(tdivs))],'L
252 ineStyle',':','Color','k');
253 set(gca,'XTick',0:10:max(ts),'YTick',0:.1:max(kgrowthsl));
254 xlabel('Time(hrs)');ylabel('Growth Rate (hr-1)');
255 subplot(212)
256 map=2.5;
257 area(tss,map*tsers,'FaceColor',0.9*ones(1,3),'EdgeColor','none');hold
258 on;
259 plot(ts,Ap,'r');xlim([0 max(ts)]);ylim([0 map]);
260 line([tdivs;tdivs],[zeros(1,numel(tdivs));map*ones(1,numel(tdivs))],'L
261 ineStyle',':','Color','k');
262 set(gca,'XTick',0:10:max(ts));box on;
263 xlabel('Time(hrs)');ylabel('[0A~P] (\muM)');
264
265 function pars=setpars
266 %Phosphorelay Parameters
267 kb=5e3;kb2=1*kb;
268 ks=12;ksd=1;
269 k1=500;k2=300;k3=.5e3;k4=200;k5=800;
270 k6=200;k7=800;
271 k8=100;k9=100;k10=100;k11=100;
272 kdpa=2;kpa=0.05;
273 kdeg0=0.3;kdil=0.1;
274
275 vb=0.3;vr=0.075;ve=0.03;
276 vk=0.9;fk=1.5;Kk=.025;nk=1;
277 vf=.15;f0F=3;K0F=.15;nf=2;
278 va=1.5;f0A=6;K0A=0.35;na=2;
279 ngk=1;ngf=1;
280
281 pars=[vk,vf,vb,va,ks,ksd,kb,kb2,k1,k2,k3,k4,k5,k6,k7,k8,k9,k10,k11,kdi
282 l...
283     f0F,K0F,nf,f0A,K0A,na,fk,Kk,nk,vr,ve,kdpa,...
284     kdeg0,kpa,ngk,ngf];
285
286 function dx=eqnsint(~,x,pars)
287
288 pars=num2cell(pars);

```

```

289 [vk, vf, vb, va, ks, ksd, kb, kb2, k1, k2, k3, k4, k5, k6, k7, k8, k9, k10, k11, kdil, ...
290 f0F, K0F, nf, f0A, K0A, na, fk, Kk, nk, vr, ve, kdpa, ...
291 kdeg0, kpa, ngk, ngf]=deal (pars{:});
292
293 kdeg=kdeg0+kdil; kb3=kb;
294
295 Kt=x (1) ; Ft=x (2) ; Bt=x (3) ; At=x (4) ; Rt=x (5) ; Et=x (6) ;
296 Kp=x (7) ; KpF=x (8) ;
297 Fp=x (9) ; KF=x (10) ;
298 Bp=x (11) ; FpB=x (12) ;
299 Ap=x (13) ; BpA=x (14) ;
300 FpR=x (15) ; ApE=x (16) ;
301 sKt=x (17) ; sFt=x (18) ; sBt=x (19) ; sAt=x (20) ;
302
303 K=max (Kt-Kp-KpF-KF) ; F=max (Ft-Fp-KpF-KF-FpB-FpR) ;
304 B=max (Bt-Bp-FpB-BpA) ; A=max (At-Ap-BpA-ApE) ;
305 R=max (Rt-FpR) ; E=max (Et-ApE) ;
306
307 vkp=vk+fk*Ap^nk/ (Kk^nk+Ap^nk) ;
308 vfp=vf+f0F*Ap^nf/ (K0F^nf+Ap^nf) ;
309 vap=va+f0A*Ap^na/ (K0A^na+Ap^na) ;
310
311 dx (1) =ngk*sKt-kdeg*Kt;
312 dx (2) =ngf*sFt-kdeg*Ft;
313 dx (3) =ngk*sBt-kdeg*Bt;
314 dx (4) =ngk*sAt-kdeg*At;
315 dx (5) =vr-kdeg*Rt;
316 dx (6) =ve-kdeg*Et;
317
318 dx (7) =ks*K-ksd*Kp-kb*Kp*F+k1*KpF-kdeg*Kp;
319 dx (8) =kb*Kp*F- (k1+k2+kdeg) *KpF+kb3*K*Fp;
320 dx (9) =k2*KpF-kdeg*Fp-kb*Fp*B+k4*FpB-kb*Fp*R+k8*FpR-kdpa*Fp-kb3*K*Fp;
321 dx (10) =kb2*K*F- (k3+kdeg) *KF;
322 dx (11) =-kdeg*Bp-kb*F*Bp+k5*FpB-kb*A*Bp+k6*BpA;
323 dx (12) =kb* (Fp*B+Bp*F) -FpB* (kdeg+k4+k5) ;
324 dx (13) =-kdeg*Ap-kb*B*Ap+k7*BpA-kb*Ap*E+k10*ApE-kdpa*Ap+kpa*A;
325 dx (14) =kb* (Ap*B+Bp*A) -BpA* (kdeg+k6+k7) ;
326 dx (15) =kb*Fp*R- (k8+k9+kdeg) *FpR;
327 dx (16) =kb*Ap*E- (k10+k11+kdeg) *ApE;
328
329 ep=1.*kdeg;
330 dx (17) =ep* (vkp-sKt) ;
331 dx (18) =ep* (vfp-sFt) ;
332 dx (19) =ep* (vb-sBt) ;
333 dx (20) =ep* (vap-sAt) ;
334 dx=dx' ;
335
336

```

#### 337 4. Appendix Text A2: Population Dynamics Model of Growth and Sporulation

338 To understand the effect of glucose addition on cell growth rate dynamics and thereby  
 339 sporulation (Fig. 3C-F), we built a simple population dynamics model. We assumed that  
 340 cell growth rate during starvation follows Monod kinetics (Kovarova-Kovar and Egli,  
 341 1998). Based on the observation of (Veening et al., 2008), we also assumed that cell  
 342 death/sporulation releases nutrients that can be reused for cell growth. Our model is  
 343 given by two equations for the number of cells (N) and amount of substrate (S):

$$344 \quad \frac{dN}{dt} = \left[ v_m \frac{S}{K_m + S} - \frac{k_d}{1 + (S/K_s)^m} \right] N$$

$$\frac{dS}{dt} = -\gamma \left[ v_m \frac{S}{K_m + S} - \frac{k_d}{1 + (S/K_s)^m} \right] N$$

345 Here  $v_m$  and  $K_m$  are the maximum growth rate and the half-maximal substrate  
 346 concentration for the Monod growth kinetics, respectively. To model the growth  
 347 threshold-based sporulation decision, we assumed that sporulation rate is a non-linear  
 348 function of the available substrate concentrations.  $k_d$ ,  $K_s$  and  $m$  are the maximum  
 349 sporulation/death rate, half-maximal concentration and the Hill-exponent, respectively.  
 350 Parameter  $\gamma$  is the substrate yield. These model parameters along with the initial  
 351 substrate concentration (arbitrary units: amt. substrate) were determined by fitting the  
 352 model to data for cell growth from time-lapse experiments in Resuspension Media. The  
 353 Levenberg-Marquardt algorithm of MATLAB *fsolve* function was used for fitting. The  
 354 initial cell number was fixed to 5. The parameter values determined from fitting are  
 355 shown in Table A3. Using these same values for parameters, the model was used to  
 356 explain the effect of increased nutrient availability at the start of the experiment.

357 As shown in Appendix Fig. 1, this model shows that the dynamics of cell growth  
 358 are sensitive to the initial substrate availability. In regular sporulation media, substrate  
 359 availability is low from the start of the experiment. As a result, cells grow slowly and the  
 360 nutrient levels are accordingly depleted gradually until the cells cross the growth  
 361 threshold for sporulation around 10 hours into the experiment (Appendix Fig. 1A). In  
 362 contrast, the addition of 0.025% glucose at the start of the experiment increases the  
 363 initial substrate availability and postpones starvation (Appendix Fig. 1B). Under these  
 364 conditions cells grow rapidly and multiply. The increased number of cells at the onset of  
 365 starvation results in a rapid depletion of nutrients and a decrease in growth rate  
 366 (Appendix Fig. 1B). Consequently, in these conditions the cells start to sporulate earlier:  
 367 around 7 hours into the experiment (Fig. 3B).

368

369 *Matlab code for Population Dynamics Model of Growth and Sporulation*

```

370
371 function BacillusPopGrowthModel
372 clc;clear;format('compact');
373 close all;
374
375 yield=0.02;Vm=1.13;Km=0.82;m=1;
376 kd=0.1;Ks=0.5;md=3.5;
377 s0RMglu=0.72;s0RM=0.44;n0=5;
378 par0=[yield,Vm,Km,m,kd,Ks,md];
379
380 tspan=[0 30];
381
382 [t,y]=ode45(@eqns,tspan,[n0 s0RM],[],par0);
383 N=y(:,1);S=y(:,2);kgRM=Vm*S.^m./(Km^m+S.^m);
384
385 figure(1)
386 subplot(221)
387 plot(t,kgRM,'k');hold on;axis square;
388 xlim([0 30]);ylim([0 0.8]);
389 xlabel('Time(hrs)');ylabel('Growth rate (hr-1)');title('RM');
390
391 [t,y]=ode45(@eqns,tspan,[n0 s0RMglu],[],par0);
392 N=y(:,1);S=y(:,2);kgRMglu=Vm*S.^m./(Km^m+S.^m);
393
394 subplot(222)
395 plot(t,kgRMglu,'r');hold on;axis square;
396 xlim([0 30]);ylim([0 0.8]);
397 xlabel('Time(hrs)');ylabel('Growth rate (hr-1)');
398 title('RM+0.025%Glu');
399
400 function dydt=eqns(t,x,pars)
401 yield=pars(1);Vm=pars(2);Km=pars(3);m=pars(4);
402 kd=pars(5);Ks=pars(6);md=pars(7);
403 N=x(1);S=x(2);
404
405 dydt(1)=(Vm*S.^m/(Km^m+S)-kd/((S/Ks)^md+1))*N;
406 dydt(2)=-yield*(Vm*S.^m/(Km^m+S.^m)-kd/((S/Ks)^md+1))*N;
407 dydt(2)=logical(S>0)*dydt(2);
408
409 dydt=dydt';

```

```

410
411

```

#### 4. Appendix References

```

412

```

```

413
414 Eswaramoorthy, P., D. Duan, J. Dinh, A. Dravis, S. N. Devi and M. Fujita (2010). "The threshold level of
415 the sensor histidine kinase KinA governs entry into sporulation in Bacillus subtilis." J Bacteriol 192(15):
416 3870-3882.

```

417 Fujita, M. and Y. Sadaie (1998). "Feedback loops involving Spo0A and AbrB in in vitro transcription of the  
418 genes involved in the initiation of sporulation in *Bacillus subtilis*." J Biochem **124**(1): 98-104.  
419 Grimshaw, C. E., S. Huang, C. G. Hanstein, M. A. Strauch, D. Burbulys, L. Wang, J. A. Hoch and J. M.  
420 Whiteley (1998). "Synergistic kinetic interactions between components of the phosphorelay controlling  
421 sporulation in *Bacillus subtilis*." Biochemistry **37**(5): 1365-1375.  
422 Hoch, J. A. (1993). "Regulation of the phosphorelay and the initiation of sporulation in *Bacillus subtilis*."  
423 Annu Rev Microbiol **47**: 441-465.  
424 Levine, J. H., M. E. Fontes, J. Dworkin and M. B. Elowitz (2012). "Pulsed feedback defers cellular  
425 differentiation." PLoS Biol **10**(1): e1001252.  
426 Narula, J., A. Kuchina, D. Y. Lee, M. Fujita, G. M. Suel and O. A. Igoshin (2015). "Chromosomal  
427 Arrangement of Phosphorelay Genes Couples Sporulation and DNA Replication." Cell **162**(2): 328-337.  
428 Weir, J., M. Predich, E. Dubnau, G. Nair and I. Smith (1991). "Regulation of spo0H, a gene coding for the  
429 *Bacillus subtilis* sigma H factor." J Bacteriol **173**(2): 521-529.